Location and mapping of the human rostromedial tegmental nucleus and associated midbrain inhibitory nuclei regulating dopamine neurons

Anastasia Filimontseva[1,2], ORCID 0000-0002-3316-9035 email afil9180@uni.sydney.edu.au

YuHong Fu[1,2], ORCID 0000-0003-4539-2039 email yuhong.fu@sydney.edu.au

Glenda M Halliday[1,2,#] ORCID 0000-0003-0422-8398 email glenda.halliday@sydney.edu.au

[1]The University of Sydney Brain and Mind Centre & Faculty of Medicine and Health School of Medical Sciences, Sydney, NSW 2050, Australia

[2]Aligning Science Across Parkinson's (ASAP) Collaborative Research Network, Chevy Chase, MD, 20815

[#]Corresponding author: Professor Glenda Halliday, University of Sydney Brain and Mind Centre, 97 Church Street, Camperdown, NSW 2050 AUSTRALIA, Email: glenda.halliday@sydney.edu.au, Tel: +61 2 9351 0888

Running title: The human rostromedial tegmental nucleus

Number of text words: 3,551

Number of figures: 5 plus 3 supplementary figures and 2 supplementary tables

Acknowledgements

The authors acknowledge: Heidi Cartwright for assistance with the figures; human brain tissue sample procurement by the Sydney Brain Bank, Sydney (enabled by funding from Neuroscience Research Australia and is a special gift in memory of Jim Raftos from the Shaw family) and Flinders Medical Centre and Institute of Medical and Veterinary Sciences, Adelaide; the use of Microscopy Australia infrastructure at the Sydney Microscopy and Microanalysis facility, University of Sydney (enabled by the National Collaborative Research Infrastructure Strategy);

and funding support by Aligning Science Across Parkinson's [020505] through the Michael J. Fox Foundation for Parkinson's Research and the National Health and Medical Research Council of Australia to GMH [Investigator Grant 1176607]. For open access, the authors have applied a CC BY public copyright license to all Author Accepted Manuscripts arising from this submission.

Abstract

Background: Animal experiments reveal distinct GABAergic cell clusters within the dopaminergic midbrain regions in the rostromedial tegmental nucleus (RMTg) and retrorubral fields (RRF) that have yet to be clearly defined in humans. These neurons send prominent inhibitory projections to dopaminergic neurons in the substantia nigra and ventral tegmental area that impact motor, reward and threat processing.

Objective: To identify GABergic RMTg and RRF cell clusters in the human brain.

Methods: Ten µm formalin-fixed paraffin-embedded transverse human brainstem sections from ten control cases were obtained from the Sydney Brain Bank and immunohistochemistry for GABA and tyrosine hydroxylase was used to determine the location and cell size of RMTg and RRF GABAergic neurons. These cell populations were further mapped in transverse 50µm thick cresyl violet stained serial midbrain sections (every 750µm) from previously published controls (Halliday et al. 1990a).

Results: GABAergic neurons were cytoarchitecturally distinct, with the largest GABAergic neurons in the RRF, followed by RMTg neurons which were larger than GABAergic neurons in the interpedunclular nucleus (Kruskal-Wallis test, $p<0.0001$). RMTg and RRF GABAergic neurons first appear in caudal transverse midbrain sections approximately 38mm above the obex. RMTg moves rostrally and medially from underneath the decussation of the superior cerebellar peduncle to just lateral to the interpeduncular nucleus. The RRF cluster also moves rostrally and medially to the parabrachial pigmented nucleus (PBP) just under the red nucleus.

Conclusion: The GABAergic neurons in RMTg and RRF/PBP that modulate dopamine neuronal excitability have distinct morphologies in humans. Identifying these inhibitory neurons is key to evaluating their role in neurodegenerative diseases.

Key words: dopaminergic neurons, GABAergic neurons, parabrachial pigmented nucleus, rostromedial tegmental nucleus, retrorubral fields, three-dimensional reconstruction

Introduction

The majority of somatodendritic inputs to dopamine (DA) neurons in the substantia nigra pars compacta (SNpc) are GABAergic (~40-70% of neurons)(Bolam and Smith 1990; Henny et al. 2012). These inhibitory afferents arise from a number of sources, some extrinsic to the SNpc (e.g. from the periaqueductal gray, dorsal raphe, lateral habenula, and basal ganglia)(Omelchenko and Sesack 2010; Beier et al. 2015; Nieh et al. 2015; Hjelmstad et al. 2013; Lerner et al. 2015; Evans et al. 2020; Vounatsos and Gittis 2025b), while others more recently defined are interspersed within the midbrain DA regions.

The main midbrain DA regions are the SNpc, retrorubral fields (RRF) and ventral tegmental area (VTA), with the VTA cytoarchitecturally subdivided into the more lateral parabrachial pigmented nucleus (PBP), medial paranigral (PN) and parainterfascicular (PIF) nuclei, and midline interfascicular (IF), central linear (CL) and rostral linear (RL) nuclei (Fu et al. 2012). Within these DA regions, the RRF has the highest proportion of GABA to DA neurons compared to other midbrain DA clusters (Nair-Roberts et al. 2008; Vounatsos and Gittis 2025b; Kelly et al. 2022). In contrast only around 29% of SNpc neurons are GABAergic, which is the lowest proportion among the main DA regions, and the VTA has a moderate population of GABAergic neurons (Nair-Roberts et al. 2008). The highest densities of GABAergic neurons in the VTA are in the caudal PN and PIF subnuclei (Nair-Roberts et al. 2008), although the rostromedial tegmental nucleus (RMTg) has not been identified in humans but in other species it is a GABAergic nucleus in ‘the tail of the VTA’ (Barrot et al. 2012).

Many GABAergic neurons intermixed within these DA regions are local interneurons. In contrast, GABAergic neurons broadly innervating midbrain DA neurons concentrate only in the RMTg and RRF (Barrot et al. 2012; Smith et al. 2019; Vounatsos and Gittis 2025a). The RMTg was initially defined in rodents with retrograde injections into the SNpc and VTA which reliably identified this concentration of GABAergic neurons (Smith et al. 2019; Jhou et al. 2009a;

Lammel et al. 2012). In addition to its direct inhibition of the motor nigrostriatal DA pathway (Bourdy et al. 2014), the RMTg in general encodes negative prediction errors and plays a critical role in behavioural inhibition in general, as well as punishment learning through mesolimbic DA pathways (Jhou 2021). As discussed above, of the midbrain DA regions the RRF has the highest concentration of GABAergic neurons which densely innervate the SNpc, although their function is less well defined (Vounatsos and Gittis 2025a). In gerbils, the RRF GABAergic pathway is involved in male sex behaviour (Simmons et al. 2011) with RRF projections in general involved in reward processing, motivation and threat evaluation (Moaddab and McDannald 2021; Vounatsos and Gittis 2025a).

Due to species differences in midbrain anatomy and neural identification using developmental markers (e.g. some transcription factors for RMTg neurons are only expressed in embryonic tissue and not in adult human brain (Allen Institute for Brain Science 2010)), the human RMTg has yet to be defined and GABAergic clusters in the human RRF have largely been ignored. The fact that there are multiple GABAergic populations in close proximity within these anatomical regions (Margolis et al. 2012) further complicates the identification of these important GABergic neuronal nuclei in the human midbrain. However, the comparative identification of these inhibitory neurons is important to determine as these midbrain nuclei provide broad inhibition to midbrain DA neurons with any deficits likely to have significant impact.

For the first time we mapped the RMTg and a large RRF GABAergic neuronal cluster (LatC) in the human brainstem using immunohistochemistry and three-dimensional reconstructions in serial sections showing that these GABAergic cell clusters have distinct morphological features and anatomical locations. Overall, we present detailed anatomical maps of these prominent human midbrain GABAergic nuclei that innervate midbrain DA neurons.

Materials and Methods

Human brain tissue

For immunohistochemical analysis, formalin-fixed paraffin-embedded (FFPE) cross-sectional midbrain tissue blocks from healthy controls without neurological or neuropathological diseases were obtained from the Sydney Brain Bank (n=10, for details see Supplementary Table 1). Serial section reconstruction using thick cross-sectional Nissl-stained midbrain sections from control

cases (n=4, for details see Supplementary Table 1) previously processed and published (Halliday et al. 1990b) were also included. These midbrain sections were cut at 50µm on a freezing microtome, collected at 750µm intervals, and stained with 0.5% cresyl violet (HB5608 Hello Bio), as previously described (Halliday et al. 1990b). The study was approved by the University of Sydney Human Research Ethics Committee (2021/845).

Immunohistochemistry

FFPE tissue blocks were sectioned at 6µm and dried on microscope slides at 37°C for 48 hours. Sections were deparaffinized by incubation at 60°C for 1 hour and then submerged in D-Limonene (Hurst Scientific, HISTO-5LCTN) for 2 x 7 minutes, followed by rehydration in decreasing ethanol concentrations (100% ethanol for 2 x 3 minutes, 95% ethanol for 3 minutes, 70% ethanol for 3 minutes) and distilled H2O for 3 minutes. Sections underwent heat-induced antigen retrieval (HIAR) in commercially available antigen retrieval solution (Invitrogen, 00-4956-58) diluted to 1x using a programmable antigen retrieval cooker (Aptum Biologics Ltd, UK, Retriever 2100). Peak temperature reached ~121°C and afterwards sections were gradually cooled for two hours. Sections were washed with tris-buffered saline (TBS, Sigma-Aldrich, 94158-10TAB), and endogenous alkaline phosphatase (AP) and hydrogen peroxidase (HRP) were quenched with BLOXALL blocking solution (SP-6000-100) for 30 minutes. Afterwards sections were blocked for 1 hour at room temperature with in-house made normal horse serum blocking solution (2% horse serum, 1% BSA in 0.01M TBS). Sections were incubated with a primary cocktail of antibodies to tyrosine hydroxylase (TH, rabbit polyclonal IgG, AB152 Sigma-Aldrich diluted 1:200) and GAD67 (mouse monoclonal IgG_3, sc-28376 Santa-Cruz Biotechnology diluted 1:50) for 4 nights at 4°C. Secondary antibody incubation for 90 minutes at room temperature used a cocktail of ImmPRESS™-alkaline phosphatase (AP) horse anti-mouse IgG polymer detection kit (MP-5402 Vector Laboratories) and ImmPRESS™-horseradish peroxidase (HRP) horse anti-rabbit IgG polymer detection kit (MP-7401 Vector Laboratories). Antibody detection was visulaised using SignalStain® Vibrant Red AP Substrate Kit (76713 Cell Signaling) and ImmPACT® DAB EqV HRP Substrate Kit (SK-4103 Vector Laboratories). Sections then underwent standard dehydration in increasing graded ethanol concentrations and cleared in xylene, prior to mounting with Eukitt® quick-hardening mounting medium (03989 Sigma-Aldrich). In separate control experiments where either the primary or secondary antibodies were omitted,was no AP or HRP was detectable.

Image acquisition

An automated slide scanner (SLIDEVIEW VS200, Tokyo, Japan) was used to scan the sections using pre-set focusing and exposure parameters. The method for brightfield image acquisition has previously been described (Filimontseva et al. 2025) with slight amendments to optimize the exposure settings for 1) the GABA and TH stained sections, and 2) for serial Nissl stained sections.

Anatomical mapping

Midbrain DA regions were cytoarchitecturally mapped on digitized images in Adobe Photoshop (ver. 25.9.1, Adobe Systems Inc., San Jose, CA, USA) and Illustrator (ver. 28.5, Adobe Systems Inc., San Jose, CA, USA) based on the human brainstem atlas and previously published cytoarchitecture studies (Paxinos et al. 2020; McRitchie et al. 1995; McRitchie et al. 1997). For the GABA and TH stained sections, TH staining was used to determine the DA brain regions and for the serial Nissl stained sections, neuromelanin pigment was used to determine the DA brain regions. To determine cytoarchitectural landmarks for the RMTg, published anatomical maps from rodents and non-human primates were used (Supplementary Figures 1-3) and the most frequent landmarks determined (Supplementary Table 2). GABA and TH stained thin sections were used to identify other relevant GABAergic neuronal clusters. Both thick and thin sections were used to reconstruct proposed three-simensional models of the DA and GABA regions of interest. The midline and aqueduct were used to align every other 50µm, taken at 750µm intervals. Landmarks were outlined and relevant clusters colour coded in Adobe Photoshop. Stacked Nissl and GABA stained sections were compiled in Adobe Illustrator, and mapped structures compared.

Quantification

A semi-automated method was used to perform morphological analysis of identified GABAergic neuronal clusters. Images of Nissl stained and GABA stained sections were loaded into QuPath (Bankhead et al. 2017) and the system trained to identify neurons in the region of interest based on stain intensity. Successful training was used to create a pixel classifier and identified neurons were filtered by size and shape. Due to technical challenges of successful GABA staining on human FFPE tissue, six cases with conspicuous GABA neuronal staining out of the total ten cases used for mapping were selected for this analysis. The morphological features of Nissl

stained neurons in the regions of interest were analysed between 33mm to 38mm Obex at every 1.6mm interval.

Statistical analysis

Statistical analyses were performed in GraphPad Prism (version 10.0.3, GraphPad Software Inc., California, United Stated). Kruskal-Wallis non-parametric test was used to compare cell circularity of neurons in the GABAergic cell cluster of the RMTg, RRF and interpeduncular nucleus in Nissl and GABA stained sections. A two-way ANOVA was run to analyse effect of anatomical region and tissue stain on neurnal size, followed by post-hoc Tukey tests. The proportion and density of GABA to Nissl neurons in the GABAergic cell clusters was also analysed with two-way ANOVA tests. For all analysis the statistical significance was set to p-value < 0.05.

Results

Comparative landmarks to identify the human RMTg

We identified comparative cytoarchitectural landmarks for the human RMTg based on animal mapping literature (Supplementary Table 2). These important landmarks from this literature oriented our anatomical search for the RMTg in human midbrain tissue sections (Supplementary Table 2). The RMTg in other species first appears at the level of caudal interpeduncular nucleus, posterior to PN (Supplementary Figure 1)(Jhou et al. 2009b; Kaufling et al. 2009). As the superior cerebellar peduncle appears, the RMTg shifts dorsally (Supplementary Figure 2). The RMTg is elongated at this level where it shifts laterally below the RRF.

Morphological identification of distinct inhibitory cell clusters in the human midbrain DA regions

Prominent distinct inhibitory neuronal clusters were identified in the RRF (an obvious novel GABAergic neuronal cell cluster we call LatC) and RMTg and were compared morphologically to GABAergic neurons in the interpeduncular nucleus (Figure 1). GABAergic neurons in these cell clusters appeared to be morphologically different, with the RRF LatC GABAergic neurons larger, rounder and more densely labelled (Figure 1f) compared to the small-medium sized RMTg GABAergic neurons that stained lighter and were randomly oriented (Figure 1e). The size

of GABAergic neurons in these cell clusters were compared to those in the interpeduncular nucleus (Figure 1a-f) revealing a significant difference between anatomical region [$F(2,10796) = 166.9$, $p<0.0001$]. Post-hoc Tukey tests revealed that RRF LatC GABAergic neurons were significantly larger than RMTg GABAergic neurons, with both being significantly larger than GABAergic neurons in the interpeduncular nucleus (Figure 1g). Analysis of neuronal size in Nissl versus GABA stained sections (Figure 1a-f) revealed a significant main effect of the stain used on neuronal size [$F(1,10796) = 21.41$, $p<0.0001$]. Further, there was a significant difference in neuronal size between anatomical region depending on the stain used [$F(2,10796) = 31.60$, $p<0.0001$]. GABAergic neurons in the interpeduncular nucleus were smaller on average than Nissl stained interpeduncular neurons, whereas the reverse was true for the RMTg and RRF LatC GABAergic neurons (Figure 1g). Cell circularity measurements confirmed that RRF LatC neurons were on average rounder than RMTg neurons [Kruskal-Wallis test, **** $p<0.0001$](Figure 1h), although not so much for the GABAergic neurons in these regions (Figure 1i). GABAergic neurons in the RRF LatC were rounder than those in the interpeduncular nucleus [Kruskal-Wallis test, * $p<0.05$](Figure 1i). The size and morphology of these concentrated midbrain GABAergic cell clusters distinguishes these different populations of midbrain GABAergic neurons.

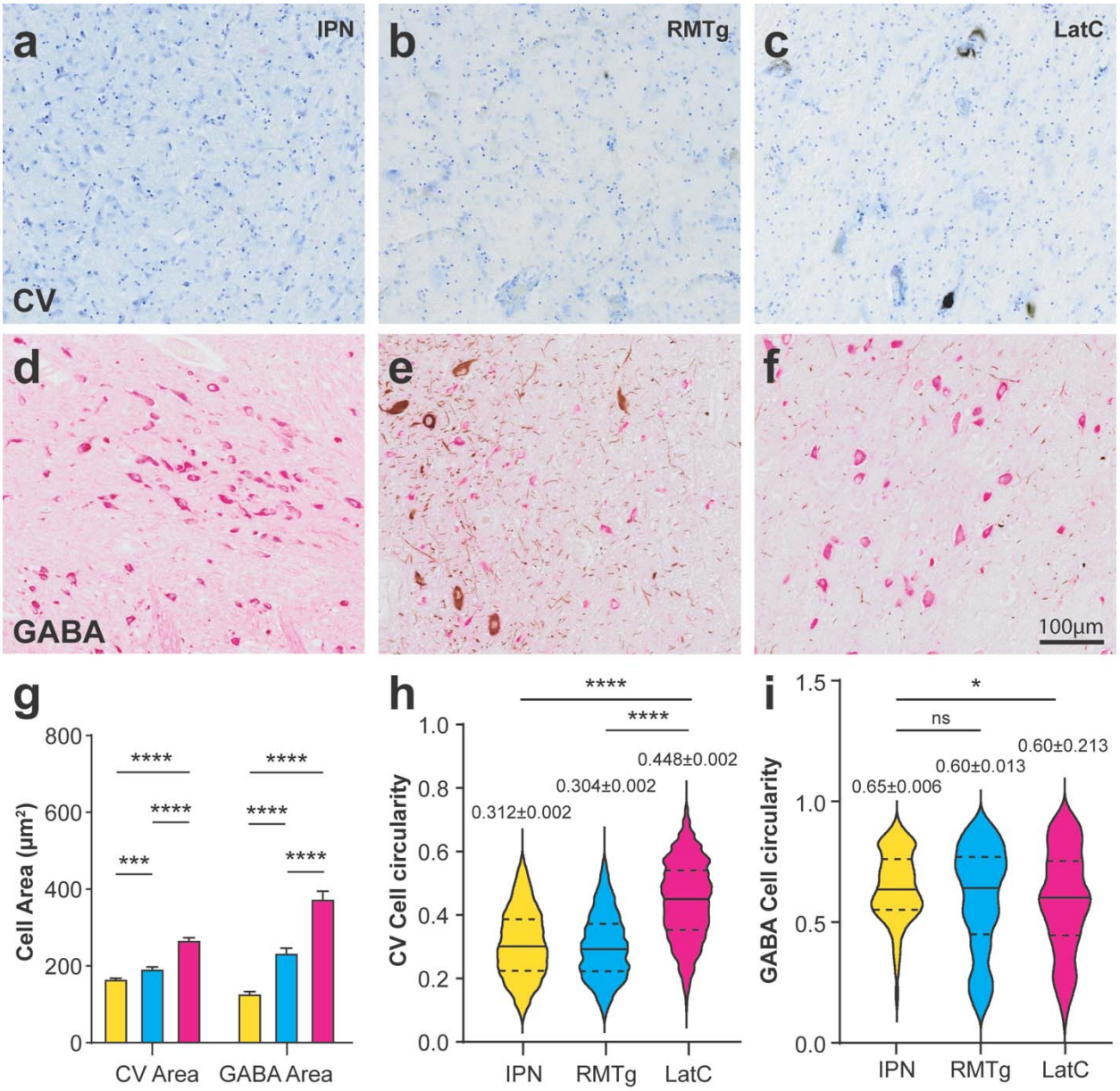

Figure 1. ***Morphological identification of distinct inhibitory clusters in the human brainstem.*** Representative images from Nissl (CV) stained serial sections (a-c) and GABA stained sections (d-f) of specific neuronal clusters. Interpeduncular nucleus (IPN) is evident in a) and d), and the rostromedial tegmental nucleus (RMTg) is presented in b) and e). A novel, lateral cluster (LatC) of GABAergic neurons in the RRF is presented in c) and f). Measures of neuronal area (g) and cell circularity (h and i) in both tissue preparations validate the identification of these distinct inhibitory neuronal cell clusters. For area analysis, a two-way ANOVA revealed that anatomic region [$F(2,10796) = 166.9$, $p<0.0001$] and stain type significantly affected neuronal size [$F(1,10796) = 21.41$, $p<0.0001$] in g). Error bars display SEM. Post-hoc Tukey tests showed that LatC neurons were the largest, **** $p<0.0001$. IPN neurons were the smallest but significantly differed in size between CV and GABA stained tissue [$F(2,10796) = 31.60$, $p<0.0001$ in g]. GABAergic neurons in IPN were slightly smaller than Nissl stained neurons, with the reverse occurring in the RMTg and RRF. Cell circularity analyses also identified differences in these neuronal cell clusters in both tissue preparations. Violin plots revealed that LatC (magenta) neurons were significantly rounder than RMTg (blue) and IPN (yellow) in CV stained sections [Kruskal-Wallis test, **** $p<0.0001$ in (h)]. GABA staining revealed significant differences only between LatC and IPN circularity [Kruskal-Wallis test, * $p<0.05$ in (i)].

Chemoarchitectural mapping of GABAergic cell clusters in midbrain DA regions

Midbrain DA regions surrounding the GABAergic RMTg and RRF LatC were cytoarchitecturally delineated and mapped using the GABA and TH colabelled sections (Figure 2). The RMTg first appeared caudally in the midbrain approximately 33-34mm above the Obex where it is at its largest in cross section mostly due to an absence of surrounding DA neurons and subregions (Figure 2). It lies lateral to the interpeduncular nucleus, dorsal to the pontine nuclei and ventromedial to the superior cerebellar peduncle (Figure 2). At these caudal levels, there is an obvious RRF LatC GABAergic cell cluster located some distance from the RMTg at the medial edge of the RRF on the ventrolateral edge of the superior cerebellar peduncle (Figure 2). In more rostral midbrain sections, the RMTg GABAergic cell cluster maintains its position but is reduced in size due to its location within the DA neurons of the VTA PN subregion and ascending DA fibres (Figure 2). The RMTg is discontinued rostrally when the dense compact SNpc occurs in cross sections (around 37mm above Obex)(Figure 2). The RRF LatC cell cluster maintains its position laterally until the VTA PBP subcluster begins to expand laterally in more rostral sections. At these levels (35-36mm above the Obex) this GABAergic cell cluster bridges between the medial RRF and lateral PBP (Figure 2). With the discontinuation of the RRF rostrally, the LatC moves ventromedially to embed into the PBP on the ventral aspect of the superior cerebellar peduncle and continues to move ventromedially to be adjacent to the RMTg within the VTA DA regions (Figure 2).

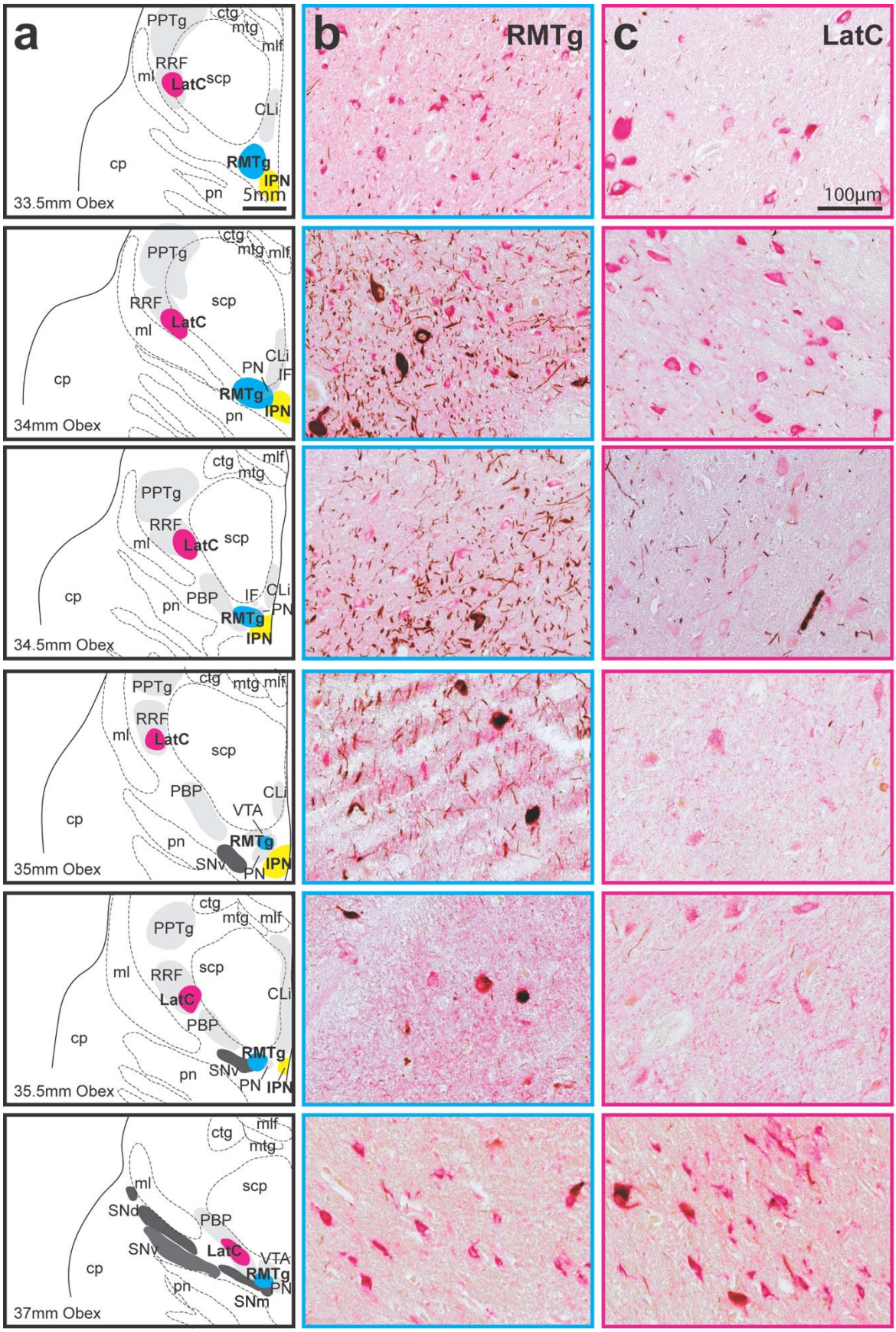
a
b
RMTg
c
LatC
PPTg
ctg
mtg
mlf
RRF
ml
LatC
scp
CLi
cp
RMTg
IPN
pn
5mm
33.5mm Obex
100µm
34mm Obex
PN
IF
34.5mm Obex
PBP
VTA
35mm Obex
SNv
35.5mm Obex
SNd
SNm
37mm Obex

259

Figure 2. ***Chemoarchitectural mapping of GABAergic cell clusters in midbrain DA regions.*** The main DA regions and landmarks were mapped in a) after immunohistochemical staining on 6µm FFPE sections. Tyrosine hydroxylase (TH)+ neurons were found in the dorsal, ventral and medial substantia nigra pars compacta (SNpc) tiers (SNd, SNv and SNM), retrorubral field (RRF), parabrachial pigmented nucleus (PBP), paranigral nucleus (PN), ventral tegmental area (VTA), caudal linear nucleus (CLi) and the interfascicular nucleus (IF). Other relevant landmarks include the pedunculopontine tegmental nucleus (PPTg), medial lemniscus (ml), superior cerebellar peduncle (scp), central tegmental tract (ctg), mammillotegmental tract (mtg), the medial longitudinal fasciculus (mlf), the interpeduncular nucleus (IPN), pontine nuclei (pn) and cerebellar peduncle (cp). Main TH+ SNpc subclusters are annotated in dark grey, whereas VTA subclusters and other relevant landmarks are shaded in light grey. Micrographs of GABA and TH immunohistochemically stained sections (GABA labeling with alkaline phosphatase in pink; TH labeled with diaminobenzidine in brown) show neurons in the RMTg and RRF/PBP LatC in b) and c) respectively. The nuclei of interest were mapped along a 4mm distance in the transverse plane. Scale bars equal 5mm in a) and 100µm in b) and c).

Cytoarchitectural identification of the RMTg and RRF LatC in midbrain DA regions

The RMTg and RRF LatC were cytoarchitecturally identified and mapped using serial thick Nissl stained cross-sectional midbrain sections to observe cell clusters more readily through a greater number of midbrain levels (Figure 3). Midbrain DA regions were identified using neuromelanin pigment. The RRF/PBP LatC was observed within the same anatomical location in these midbrain DA subregions, that is, in the medial edge of the RRF shifting in rostral sections to the dorsolateral PBP subregion (Figure 3).

The cytoarchitecture of the RMTg is highlighted in more detail as this subregion has not previously been identified cytoarchitecturally in humans. In Nissl stained midbrain sections, RMTg neurons seem smaller, more round and overall denser compared to their neighboring DA cell regions (Figure 3 and Supplementary Figure 3). Caudally the RMTg cell cluster can be identified lateral to the interpeduncular nucleus, and in more rostral sections collocates dorsal to the medial SNpc cell cluster alongside/overlapping with the VTA PN DA subregion (Figure 3).

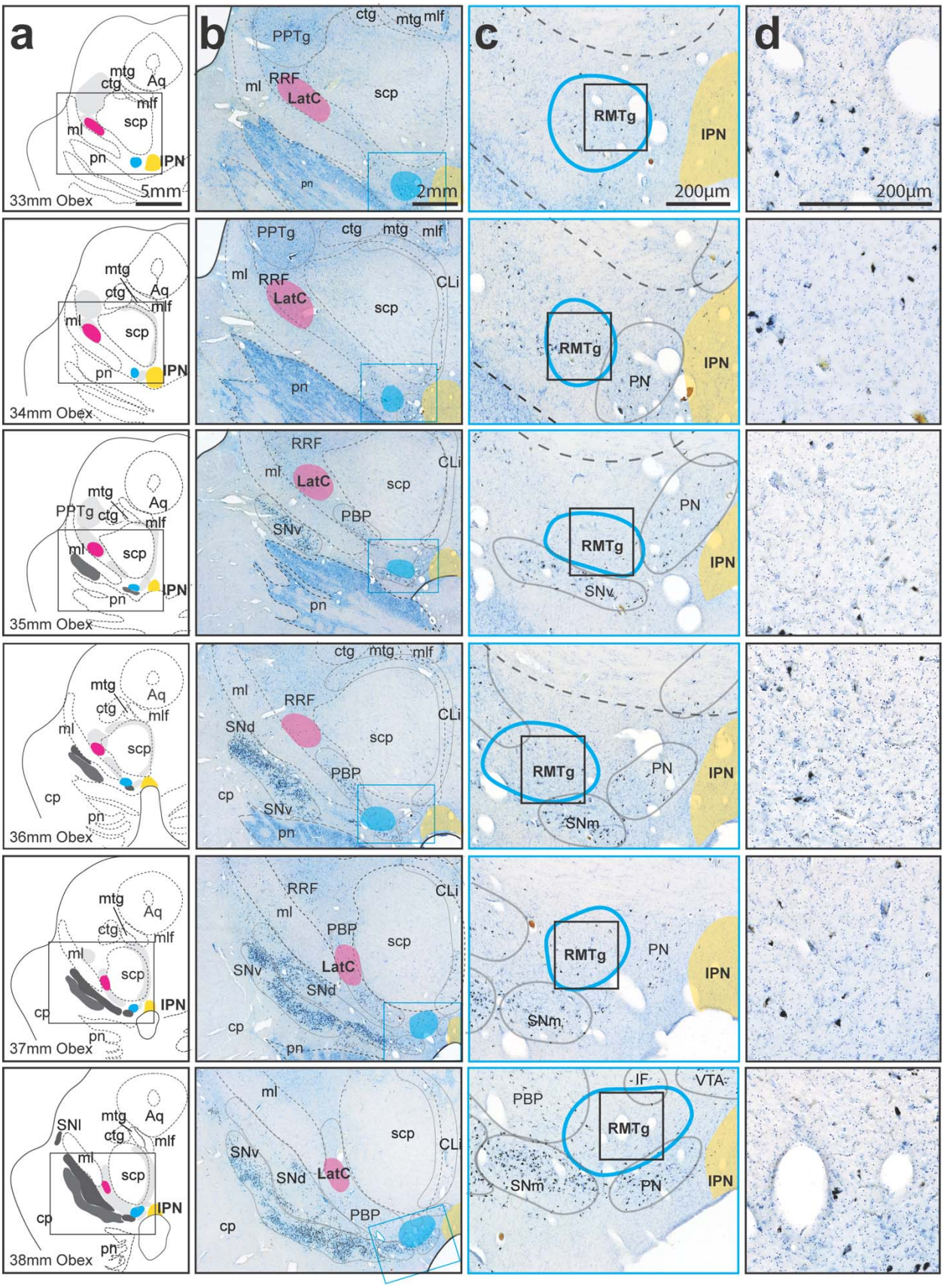
a
b
c
d
33mm Obex
34mm Obex
35mm Obex
36mm Obex
37mm Obex
38mm Obex
5mm
2mm
200µm
200µm
mtg
ctg
Aq
mlf
ml
scp
pn
IPN
PPTg
RRF
LatC
CLi
PBP
SNv
SNd
SNm
SNl
cp
PN
RMTg
IF
VTA

287

Figure 3. ***Cytoarchitectural identification of the RMTg and RRF/PBP lateral GABAergic cell cluster (LatC) in the human midbrain.*** a) Schematic mapping of 50µm-thick Nissl (CV) stained sections shown in b). Substantia nigra pars compacta (SNpc) and ventral tegmental area (VTA) subclusters, as well as retrorubral field (RRF) and other relevant nuclei (e.g. the pedunculopontine tegmental nucleus or PPTg), are annotated in grey. RRF, VTA, PPTg and several other nuclei are shown in light grey, whereas SNpc subdivisions are shaded in darker grey. The aqueduct (Aq) and fiber tracts, such as medial lemniscus (ml), superior cerebellar peduncle (scp), central tegmental tract (ctg), mammillotegmental tract (mtg) and the medial longitudinal fasciculus (mlf), are also relevant landmarks. The rostromedial tegmental nucleus (RMTg, blue) is located slightly lateral to the interpeduncular nucleus (IPN, yellow), whereas the RRF/PBP lateral GABAergic cell cluster (LatC, magenta) is much more lateral. c) Higher magnification regional micrographs of RMTg and cellular view of individual neurons in d). Scale bars equal 5mm in a), 2mm in b), 200µm in c), and 200µm in d). Abbreviations: substantianigra lateral part (SNl); medial, dorsal and ventral tiers, SNm, SNd and SNv; parabrachial pigmented nucleus (PBP); paranigral nucleus (PN); caudal linear nucleus (CLi); interfascicular nucleus (IF); pontine nuclei (pn) and cerebellar peduncle (cp).

Integrated cyto- and chemo-architectural three-dimensional (3D) model of the GABAergic cell clusters in the human RMTg and RRF/PBP

Three dimensional modelling revealed consistent overlap between the structural and chemical location of the mapped GABAergic cell clusters in both tissue types (Figure 4a). Both the RMTg and RRF/PBP LatC shift medially min the midbrain from caudal to rostral (Figure 4a). A pseudo-3D model of the RMTg and RRF/PBP LatC was constructed across cases in the rostrocaudal plane (Figure 4b). This model confirms the concentration of the RMTg to the lateral edge of the interpeduncular nucleus (Figure 4b). The larger area of the LatC in the ventromedial RRF hugs the ventrolateral edge of the superior cerebellar peduncle above and the medial lemniscus below, then travels rostomedially to the PBP and the more ventromedial aspect of the superior cerebellar peduncle (Figure 4b).

The composition and density of neurons in these GABAergic cell clusters was then determined and compared. The composition of neurons was relatively uniform in the three GABAergic neuronal regions in humans with approximately 40-60% of neurons staining with the GAD67 antibody (Figure 4c). However, the density of GABAergic neurons differs between these regions with a higher density of GABAergic neurons in the interpeduncular nucleus compared to the RMTg and LatC, and a lower density of non-GABAergic neurons in the LatC [$F(2,28) = 3.737$, * $p<0.0364$](Figure 4f). Overall our data show that there are discrete concentrations of morphologically different GABAergic neurons in two midbrain DA regions in humans, the RMTg with smaller neurons (previously identified in non-human species), and a novel more concentrated cell cluster with larger GABAergic neurons in the RRF/PBP.

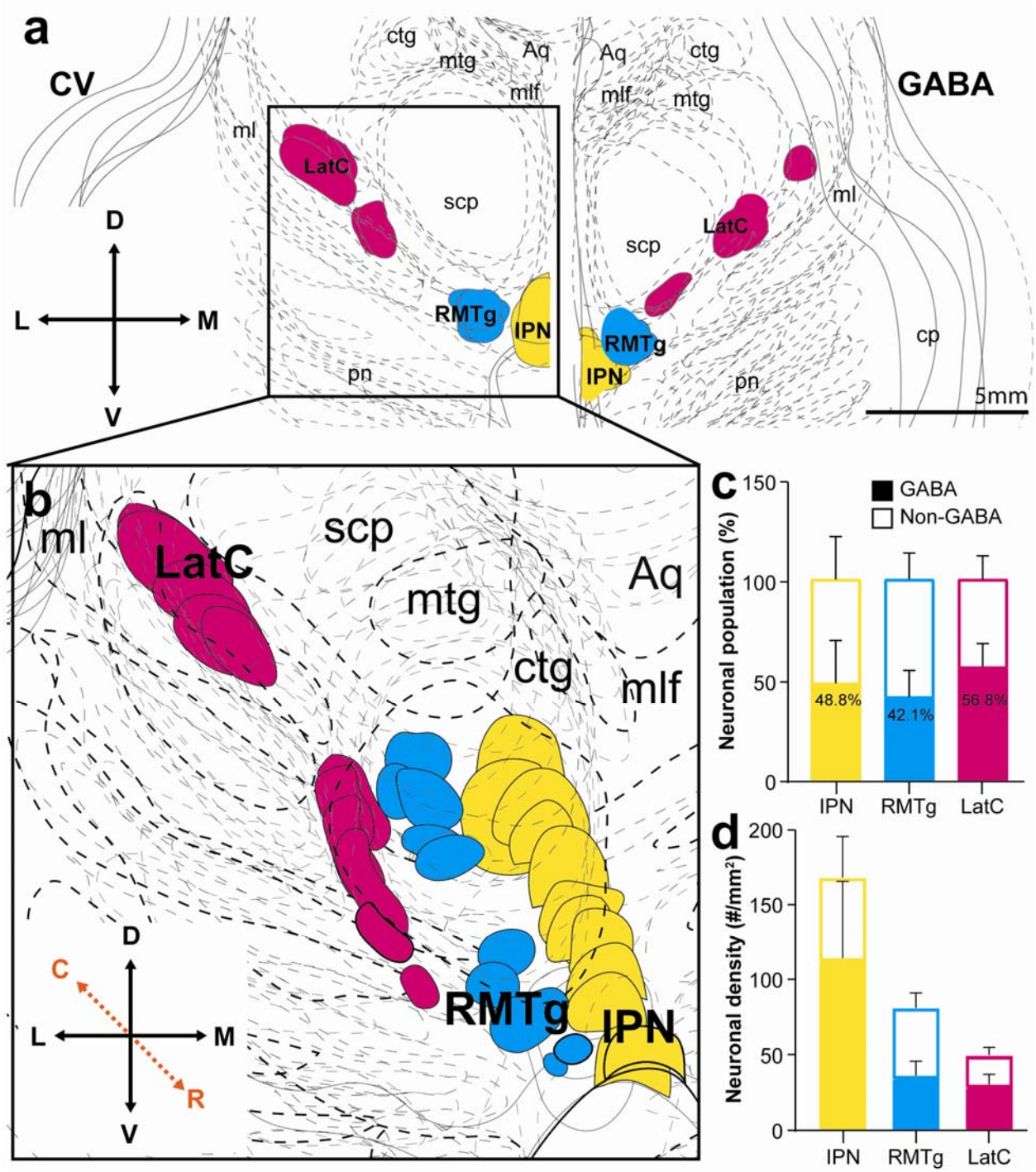

Figure 4. ***Integrated cyto- and chemo-architectural three dimensional model of the GABAergic neuronal clusters in the human midbrain DA regions.*** a) Schematic reconstructions of inhibitory nuclei of interest. Cross-sectional midbrain Nissl (CV) stained serial sections (left) and GABA-labeled sections (right) were collapsed and integrated across approximately 4-6mm in the rostrocaudal plane. Scale bar equals 5mm. To visualise a pseudo-3D transformation of these inhibitory midbrain nuclei, traced cytoarchitectural sections were aligned at a slight angle and the zoomed in region is shown in b). As expected, the rostromedial tegmental nucleus (RMTg, blue) closely associates with the interpeduncular nucleus (IPN), whereas the lateral cell cluster (LatC, magenta) shifts between the retrorubral field (RRF) and parabrachial pigmented nucleus (PBP) DA subregions. Within these GABAergic cell clusters, neuronal populations were further assessed in c) and d). Approximately half of IPN, RMTg

and LatC neurons are GABAergic in c). However, the neuronal density differs because with a significant main effect of anatomical region on cell density in d) [F (2,28) = 3.737, * p=0.0364]. Error bars display SEM in c) and d). Abbreviations: aqueduct (Aq); medial lemniscus (ml); central tegmental tract (ctg); mammillotegmental tract (mtg); medial longitudinal fasciculus (mlf); superior cerebellar peduncle (scp); pontine nuclei (pn); cerebellar peduncle (cp).

Discussion

This study identified two concentrated clusters of inhibitory neurons in the human midbrain DA regions, with one cluster equivalent to the RMTg that has been previously identified in non-human species (Figure 5a and RMTg information in Supplementary file) and the other a novel dense cluster of larger GABAergic neurons we called LatC that crosses the RRF and PBP DA subregions (Figure 5b). Morphological analyses confirmed that these two inhibitory neuronal clusters are distinct. The RMTg has not been identified in the human midbrain, and to the best of our knowledge the separate inhibitory neuronal population in the LatC has also not been identified. Approximately half of the neuronal population in these cell clusters are GABAergic with LatC having a lower density of non-GABAergic neurons compared with the RMTg. In rodents the proportion of GABAergic neurons in the RMTg is approximately 70-90% (Morello and Partanen 2015), although human brain tissue fixation may have contributed to an undercount of GABAergic neurons in our study. We used a GAD67 antibody to label cytoplasmic GABA and longer fixation can alter GAD epitopes to reduce the number of detectable GABAergic neurons (Howat and Wilson 2014; Vincek et al. 2003). However, we used antigen retrieval methods and the proportion of non-DA to DA neurons in the substantia nigra is known to be higher in rodents compared with humans (Hardman et al. 2002), with our data consistent with this orthogonal observation. Further studies are required to confirm our findings in humans and to determine the identity of the non-GABAergic neuronal population in these midbrain nuclei.

In addition to their morphological differences, these two GABAergic nuclei have been shown to be molecularly distinct developmentally in rodents (Lahti et al. 2016; Düdükcü et al. 2024). Specifically, one study has shown that *Sox14* and *Zfmp2* transcription factors distinguish developing RMTg from RRF GABAergic neurons (Lahti et al. 2016), while another study shows that *Nkx2.2* identifies three developing GABAergic subtypes in the lateral non-SNpc regions (RRF not identified directly) and that *Slc32a1* identified six developing GABAergic subtypes in the SNpc and VTA regions (two GABAergic neuron subtypes and four DA+GABA neuron

subtypes) (Düdükcü et al. 2024). This suggests that there are molecular differences between these midbrain GABAergic cell clusters which require further evaluation in humans.

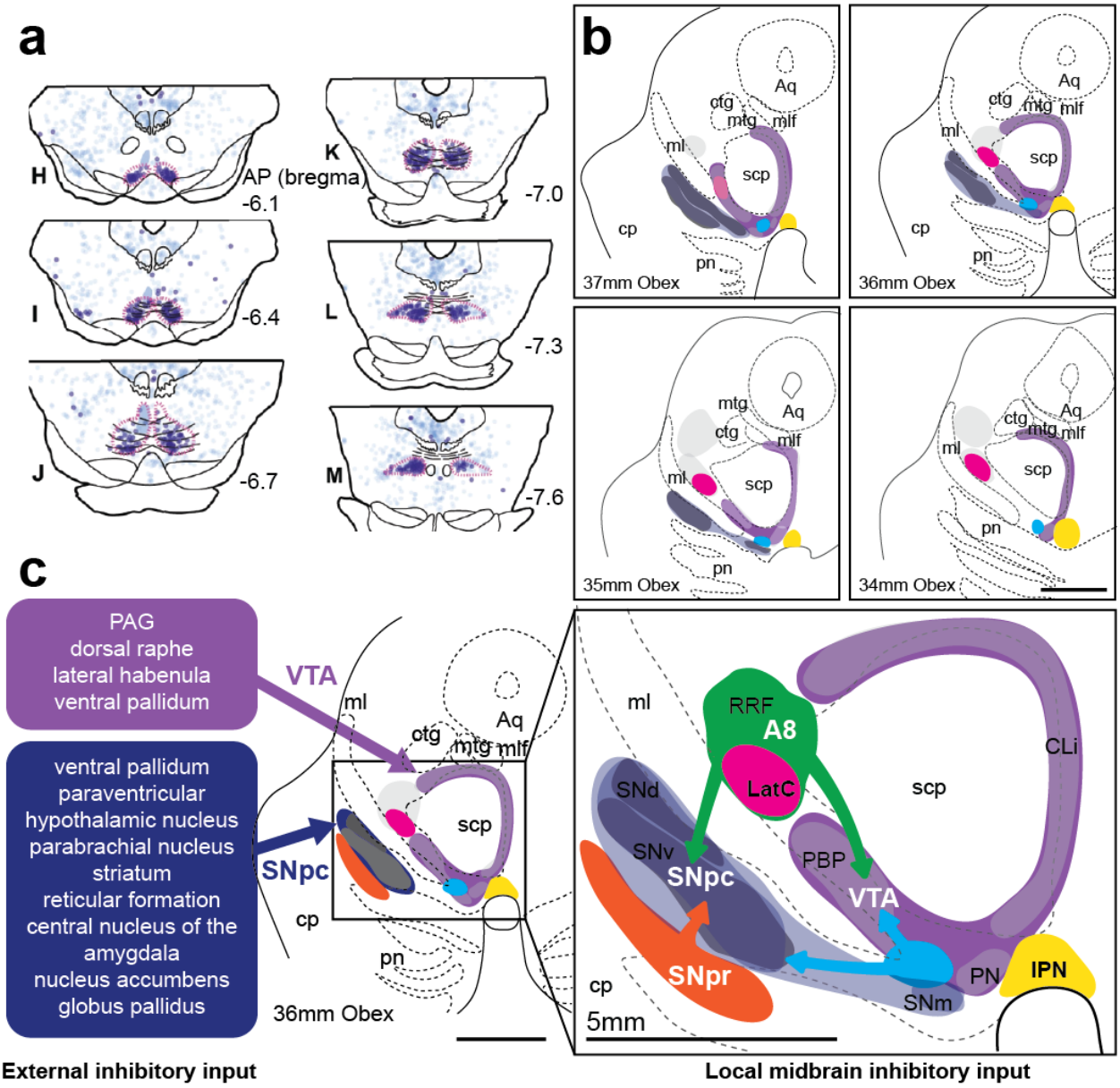

Figure 5. Connectivity of inhibitory nuclei to DA brain regions in humans. a) Rodent anatomical mapping of RMTg (red outlines of dark blue neuron representative circles among other tract traced neurons in light blue). Figure adapted and reproduced with permission from *Smith et al., 2019* (Smith et al. 2019). b) GABA and DA clusters in the caudal human midbrain showing the lateral cluster (LatC), RMTg and interpeduncular nucleus (IPN). c) Summarised inhibitory input from rodent and non-human primate connectivity literature. VTA receives input from periaqueductal gray, dorsal raphe, lateral habenula and ventral pallidum. SNpc also receives projections from the ventral pallidum, as well as other regions included in the blue box. These DA regions also receive inhibitory projections from the RMTg, substantia nigra pars reticulata (SNpr) and RRF. Scale bars equal 5mm in b) and left side c), and 2mm in right side c). Abbreviations: aqueduct (Aq); medial lemniscus (ml); superior cerebellar peduncle (scp); caudal linear (CLi); parabrachial pigmented nucleus (PBP); paranigral nucleus (PN); substantia nigra pars compacta (SNpc) lateral part, medial, dorsal and ventral tiers, SNl, SNm, SNd and SNv, respectively; central

tegmental tract (ctg); mammillotegmental tract (mtg); medial longitudinal fasciculus (mlf); cerebellar peduncle (cp); pontine nuclei (pn).

Using anatomical landmarks, we have generated three dimensional cyto- and chemo-architectural maps of the human midbrain to show the location of these inhibitory cell clusters within the DA subregions. Mapping these midbrain inhibitory nuclei in humans will enable further understanding of their molecular signatures, function and dysfunction in disease. The recent evidence that chronic hyperactivity of DA neurons in animal models leads to DA cell dysfunction and loss (Rademacher et al. 2025) makes identifying and evaluating these midbrain GABAergic nuclei important.

Differences between the midbrain inhibitory circuits

As identified in the introduction, midbrain DA neurons in the SNpc and VTA receive major GABA input from a variety of sources that can be divergent in function (Figure 5c). Midbrain projecting external inhibitory circuits differ functionally, molecularly and structurally. Genetically defined globus pallidus and dorsal striatum cells inhibit SNpc DA neurons but only striatal inputs induce rebound firing (Evans et al. 2020). Aldh1a1+ SNpc neurons receive inputs from molecularly distinct striatal clusters, which have opposite effects on locomotion (Dong et al. 2025), potentially due to their location on distal dendrites - striosomal GABAergic axons have a positive relationship between inhibition strength and distance away from the SNpc proximal dendrite (Evans et al. 2020). Evidence of functional differences in the input of GABA from the RMTg versus extrinsic sources to the VTA is that activation of RMTg GABA terminals induces place avoidance whereas PAG GABA terminal activation induces immobility (St. Laurent et al. 2020). Further work on determining how different inhibitory circuits influence DA neuronal function is required. Importantly, the inhibition exerted by RMTg GABAergic neurons on midbrain DA neurons is bigger compared to the one mediated for example by the substantia nigra pars reticulata GABA neurons (Morello and Partanen 2015), further warranting the study of these inhibitory midbrain nuclei in humans.

The identified RMTg and RRF/PBP LatC GABAergic nuclei must be functionally different from each other as well as external GABA inputs based on their location within different functional brain regions (Figure 5c). The GABAergic nuclei embedded in the DA subregions likely mediate different effects on midbrain DA neurons. Recent evidence in primates show that RRF and PBP

GABAergic neurons receive equivalent GABAergic inputs to their DA neighbours (Fudge et al. 2024). Neural circuits with such mutual inhibitory connections are able to rapidly and flexibly switch between distinct functions allowing multiple controllable functions to be managed through the same circuits (Liu et al. 2025). The demonstration of these two distinct GABAergic nuclei that receive similar afferents to their DA neighbours and innervate broadly across all DA subregions is likely to at least double the tunable flexibility of the multiple functions regulated through DA circuits. These and other inhibitory nuclei are promising anatomical correlates for unexplored biological and disease mechanisms.

Overall, this is the first study to identify RMTg and RRF/PBP LatC GABAergic nuclei in the human midbrain. The data presented show clear concentrations of large GABAergic neurons in these human midbrain regions, higher numbers than expected for the small intrinsic interneurons also found in DA subregions. Given their major input to midbrain DA neurons it will be important to understand how their interactions impacts midbrain DA motor and behavioural functions, particularly as chronic hyperactivity of DA neurons in animal models leads to DA cell dysfunction and loss (Rademacher et al. 2025).

References

Allen Institute for Brain Science (2010) Allen Human Brain Atlas. Allen Institute for Brain Science. https://human.brain-map.org. Accessed 24/10 2025

Bankhead P, Loughrey MB, Fernández JA, Dombrowski Y, McArt DG, Dunne PD, McQuaid S, Gray RT, Murray LJ, Coleman HG, James JA, Salto-Tellez M, Hamilton PW (2017) QuPath: Open source software for digital pathology image analysis. Scientific Reports 7 (1):16878. doi:10.1038/s41598-017-17204-5

Barrot M, Sesack SR, Georges F, Pistis M, Hong S, Jhou TC (2012) Braking dopamine systems: a new GABA master structure for mesolimbic and nigrostriatal functions. J Neurosci 32 (41):14094-14101. doi:10.1523/JNEUROSCI.3370-12.2012

Beier Kevin T, Steinberg Elizabeth E, DeLoach Katherine E, Xie S, Miyamichi K, Schwarz L, Gao Xiaojing J, Kremer Eric J, Malenka Robert C, Luo L (2015) Circuit Architecture of VTA Dopamine Neurons Revealed by Systematic Input-Output Mapping. Cell 162 (3):622-634. doi:10.1016/j.cell.2015.07.015

Bolam JP, Smith Y (1990) The GABA and substance P input to dopaminergic neurones in the substantia nigra of the rat. Brain Research 529 (1):57-78. doi:https://doi.org/10.1016/0006-8993(90)90811-O

Bourdy R, Sanchez-Catalan MJ, Kaufling J, Balcita-Pedicino JJ, Freund-Mercier MJ, Veinante P, Sesack SR, Georges F, Barrot M (2014) Control of the nigrostriatal dopamine neuron activity and motor function by the tail of the ventral tegmental area. Neuropsychopharmacology 39 (12):2788-2798. doi:10.1038/npp.2014.129

Dong J, Wang L, Sullivan BT, Sun L, Martinez Smith VM, Chang L, Ding J, Le W, Gerfen CR, Cai H (2025) Molecularly distinct striatonigral neuron subtypes differentially regulate locomotion. Nature Communications 16 (1):2710. doi:10.1038/s41467-025-58007-x

Düdükcü Ö, Raj DDA, van de Haar LL, Grossouw LM, Linders LE, Garritsen O, Adolfs Y, van Kronenburg NCH, Broekhoven MH, Kapteijns THW, Meye FJ, Pasterkamp RJ (2024) Molecular diversity and migration of GABAergic neurons in the developing ventral midbrain. iScience 27 (11):111239. doi:https://doi.org/10.1016/j.isci.2024.111239

Evans RC, Twedell EL, Zhu M, Ascencio J, Zhang R, Khaliq ZM (2020) Functional Dissection of Basal Ganglia Inhibitory Inputs onto Substantia Nigra Dopaminergic Neurons. Cell Rep 32 (11):108156. doi:10.1016/j.celrep.2020.108156

Filimontseva A, Cuadros T, Chatterton Z, Burke A, Mahabadian AA, Compte J, Fu Y, Vila M, Halliday GM (2025) Standardised TruAI Automated Quantification of Intracellular Neuromelanin Granules in Human Brain Tissue Sections. Neuropathol Appl Neurobiol 51 (4):e70033. doi:10.1111/nan.70033

Fu Y, Yuan Y, Halliday G, Rusznak Z, Watson C, Paxinos G (2012) A cytoarchitectonic and chemoarchitectonic analysis of the dopamine cell groups in the substantia nigra, ventral tegmental area, and retrorubral field in the mouse. Brain Struct Funct 217 (2):591-612. doi:10.1007/s00429-011-0349-2

Fudge JL, Kelly EA, Love TM (2024) Amygdalo-nigral inputs target dopaminergic and GABAergic neurons in the primate: a view from dendrites and soma. bioRxiv. doi:10.1101/2024.01.16.575910

Halliday GM, Li YW, Blumbergs PC, Joh TH, Cotton RG, Howe PR, Blessing WW, Geffen LB (1990a) Neuropathology of immunohistochemically identified brainstem neurons in Parkinson's disease. Ann Neurol 27 (4):373-385. doi:10.1002/ana.410270405

Halliday GM, Li YW, Blumbergs PC, Joh TH, Cotton RGH, Howe PRC, Blessing WW, Geffen LB (1990b) Neuropathology of immunohistochemically identified brainstem neurons in Parkinson's disease. Annals of Neurology 27 (4):373-385. doi:https://doi.org/10.1002/ana.410270405

Hardman CD, Henderson JM, Finkelstein DI, Horne MK, Paxinos G, Halliday GM (2002) Comparison of the basal ganglia in rats, marmosets, macaques, baboons, and humans: volume and neuronal number for the output, internal relay, and striatal modulating nuclei. J Comp Neurol 445 (3):238-255. doi:10.1002/cne.10165

Henny P, Brown MTC, Northrop A, Faunes M, Ungless MA, Magill PJ, Bolam JP (2012) Structural correlates of heterogeneous in vivo activity of midbrain dopaminergic neurons. Nature Neuroscience 15 (4):613-619. doi:10.1038/nn.3048

Hjelmstad GO, Xia Y, Margolis EB, Fields HL (2013) Opioid Modulation of Ventral Pallidal Afferents to Ventral Tegmental Area Neurons. The Journal of Neuroscience 33 (15):6454. doi:10.1523/JNEUROSCI.0178-13.2013

Howat WJ, Wilson BA (2014) Tissue fixation and the effect of molecular fixatives on downstream staining procedures. Methods 70 (1):12-19. doi:https://doi.org/10.1016/j.ymeth.2014.01.022

Jhou TC (2021) The rostromedial tegmental (RMTg) "brake" on dopamine and behavior: A decade of progress but also much unfinished work. Neuropharmacology 198:108763. doi:10.1016/j.neuropharm.2021.108763

Jhou TC, Fields HL, Baxter MG, Saper CB, Holland PC (2009a) The Rostromedial Tegmental Nucleus (RMTg), a GABAergic Afferent to Midbrain Dopamine Neurons, Encodes Aversive Stimuli and Inhibits Motor Responses. Neuron 61 (5):786-800. doi:https://doi.org/10.1016/j.neuron.2009.02.001

Jhou TC, Geisler S, Marinelli M, Degarmo BA, Zahm DS (2009b) The mesopontine rostromedial tegmental nucleus: A structure targeted by the lateral habenula that projects to the ventral tegmental area of Tsai and substantia nigra compacta. J Comp Neurol 513 (6):566-596. doi:10.1002/cne.21891

Kaufling J, Veinante P, Pawlowski SA, Freund-Mercier MJ, Barrot M (2009) Afferents to the GABAergic tail of the ventral tegmental area in the rat. J Comp Neurol 513 (6):597-621. doi:10.1002/cne.21983

Kelly EA, Contreras J, Duan A, Vassell R, Fudge JL (2022) Unbiased Stereological Estimates of Dopaminergic and GABAergic Neurons in the A10, A9, and A8 Subregions in the Young Male Macaque. Neuroscience 496:152-164. doi:https://doi.org/10.1016/j.neuroscience.2022.06.018

Lahti L, Haugas M, Tikker L, Airavaara M, Voutilainen MH, Anttila J, Kumar S, Inkinen C, Salminen M, Partanen J (2016) Differentiation and molecular heterogeneity of inhibitory and excitatory neurons associated with midbrain dopaminergic nuclei. Development 143 (3):516-529. doi:10.1242/dev.129957

Lammel S, Lim BK, Ran C, Huang KW, Betley MJ, Tye KM, Deisseroth K, Malenka RC (2012) Input-specific control of reward and aversion in the ventral tegmental area. Nature 491 (7423):212-217. doi:10.1038/nature11527

Lerner Talia N, Shilyansky C, Davidson Thomas J, Evans Kathryn E, Beier Kevin T, Zalocusky Kelly A, Crow Ailey K, Malenka Robert C, Luo L, Tomer R, Deisseroth K (2015) Intact-Brain Analyses Reveal Distinct Information Carried by SNc Dopamine Subcircuits. Cell 162 (3):635-647. doi:https://doi.org/10.1016/j.cell.2015.07.014

Liu B, White AJ, Lo CC (2025) Augmenting flexibility: mutual inhibition between inhibitory neurons expands functional diversity. iScience 28 (2):111718. doi:10.1016/j.isci.2024.111718

Margolis EB, Toy B, Himmels P, Morales M, Fields HL (2012) Identification of Rat Ventral Tegmental Area GABAergic Neurons. PLOS ONE 7 (7):e42365. doi:10.1371/journal.pone.0042365

McRitchie DA, Cartwright HR, Halliday GM (1997) Specific A10 Dopaminergic Nuclei in the Midbrain Degenerate in Parkinson's Disease. Experimental Neurology 144 (1):202-213. doi:https://doi.org/10.1006/exnr.1997.6418

McRitchie DA, Halliday GM, Cartwright H (1995) Quantitative analysis of the variability of substantia nigra pigmented cell clusters in the human. Neuroscience 68 (2):539-551. doi:10.1016/0306-4522(95)00163-D

Moaddab M, McDannald MA (2021) Retrorubral field is a hub for diverse threat and aversive outcome signals. Curr Biol 31 (10):2099-2110 e2095. doi:10.1016/j.cub.2021.02.055

Morello F, Partanen J (2015) Diversity and development of local inhibitory and excitatory neurons associated with dopaminergic nuclei. FEBS Letters 589 (24PartA):3693-3701. doi:https://doi.org/10.1016/j.febslet.2015.10.001

Nair-Roberts RG, Chatelain-Badie SD, Benson E, White-Cooper H, Bolam JP, Ungless MA (2008) Stereological estimates of dopaminergic, GABAergic and glutamatergic neurons in the ventral tegmental area, substantia nigra and retrorubral field in the rat. Neuroscience 152 (4):1024-1031. doi:https://doi.org/10.1016/j.neuroscience.2008.01.046

Nieh Edward H, Matthews Gillian A, Allsop Stephen A, Presbrey Kara N, Leppla Christopher A, Wichmann R, Neve R, Wildes Craig P, Tye Kay M (2015) Decoding Neural Circuits that Control Compulsive Sucrose Seeking. Cell 160 (3):528-541. doi:10.1016/j.cell.2015.01.003

Omelchenko N, Sesack SR (2010) Periaqueductal gray afferents synapse onto dopamine and GABA neurons in the rat ventral tegmental area. Journal of Neuroscience Research 88 (5):981-991. doi:https://doi.org/10.1002/jnr.22265

Paxinos G, Furlong T, Watson C (2020) Human brainstem: cytoarchitecture, chemoarchitecture, myeloarchitecture. Academic Press,

Rademacher K, Doric Z, Haddad D, Mamaligas A, Liao SC, Creed R, Kano K, Chatterton Z, Fu Y, Garcia JH, Vance VM, Sei YJ, Kreitzer A, Halliday G, Nelson AB, Margolis E, Nakamura K (2025) Chronic hyperactivation of midbrain dopamine neurons causes preferential dopamine neuron degeneration. Elife 13. doi:10.7554/eLife.98775

Simmons DA, Hoffman NW, Yahr P (2011) A forebrain-retrorubral pathway involved in male sex behavior is GABAergic and activated with mating in gerbils. Neuroscience 175:162-168. doi:10.1016/j.neuroscience.2010.11.048

Smith RJ, Vento PJ, Chao YS, Good CH, Jhou TC (2019) Gene expression and neurochemical characterization of the rostromedial tegmental nucleus (RMTg) in rats and mice. Brain Structure and Function 224 (1):219-238. doi:10.1007/s00429-018-1761-7

St. Laurent R, Martinez Damonte V, Tsuda AC, Kauer JA (2020) Periaqueductal Gray and Rostromedial Tegmental Inhibitory Afferents to VTA Have Distinct Synaptic Plasticity and Opiate Sensitivity. Neuron 106 (4):624-636.e624. doi:https://doi.org/10.1016/j.neuron.2020.02.029

Vincek V, Nassiri M, Nadji M, Morales AR (2003) A Tissue Fixative that Protects Macromolecules (DNA, RNA, and Protein) and Histomorphology in Clinical Samples. Laboratory Investigation 83 (10):1427-1435. doi:https://doi.org/10.1097/01.LAB.0000090154.55436.D1

Vounatsos MV, Gittis AH (2025a) GPe Projections to the Retrorubral Field Give Rise to Diverging GABAergic and DAergic Circuits. J Neurosci 45 (2). doi:10.1523/JNEUROSCI.1446-24.2024

Vounatsos MV, Gittis AH (2025b) GPe Projections to the Retrorubral Field Give Rise to Diverging GABAergic and DAergic Circuits. The Journal of Neuroscience 45 (2):e1446242024. doi:10.1523/JNEUROSCI.1446-24.2024

Statements & Declarations

Funding

This work was supported in part by Aligning Science Across Parkinson's [020505] through the Michael J. Fox Foundation for Parkinson's Research (MJFF) and also by funding from the National Health and Medical Research Council of Australia to GMH [Investigator Grant 1176607]. For open access, the authors have applied a CC BY public copyright license to all Author Accepted Manuscripts arising from this submission.

Competing interests

The authors declare no competing interests.

Author contributions

All authors contributed to the study conception and design. Material preparation and data collection were performed by Anastasia Filimontseva and analysis were performed by all authors. The first draft of the manuscript was written by Anastasia Filimontseva and all authors commented on previous versions of the manuscript. All authors read and approved the final manuscript.

Data availability

The data and analysis images and key lab materials used and generated in this study are listed in a Key Resource Table alongside their persistent identifiers at Zenodo DOI 10.5281/zenodo.17946370.

Ethics approval

Tissue was obtained from the Sydney Brain Bank (UNSW Sydney Human Research Ethics Committee approval HC200026) and the study approved by the University of Sydney Human Research Ethics Committee (2021/845).